Int. J. Solids Structures, 1967, Vol. 3, pp. 1023 to 1030. Pergamon Press Ltd. Printed in Great Britain

NONLINEAR BUCKLING AND SNAP-OVER OF A TWO-MEMBER FRAME

JOHN V. HUDDLESTON

State University of New York at Buffalo, Buffalo, N.Y.

Abstract—A study is made of the buckling behavior of a two-member frame, allowing for large rotations in both members. Special algorithms are devised to solve the nonlinear boundary-value problem that arises, and solutions obtained on a digital computer are plotted and compared with linearized results. Stable and unstable equilibrium configurations are distinguished, and the circumstances under which the frame snaps over onto its side are described.

INTRODUCTION

THE assumption in the analysis of stability of frames that only selected members carrying large compressive forces exhibit buckling behavior, while the rest of the members behave merely as axially-loaded beams, leads to a type of mathematical problem in which the buckling loads are determined from transcendental equations, as illustrated by Timoshenko and Gere [1]. The approximate expression normally used for the curvature in the Bernoulli–Euler formula in this approach is what linearizes the problem (giving, that is, linear differential equations to describe the deflections of the columns).

To understand the buckling and post-buckling behavior of frames in a more complete manner requires the following refinements:

(i) Recognition of the column action in all members.

(ii) Use of an exact expression for the curvature throughout.

These are made in this paper for a two-member frame, and the nonlinear boundary-value problem that results is solved by the generalization of a technique discussed elsewhere by the author [2].

Although there is a vast literature concerned with the stability of frames, most of the work done has been based on assumptions restricting the size of the deflections. This paper, while utilizing well-known numerical techniques, is believed to contain some new results, inasmuch as it does not limit the size of the displacements.

THEORY

Figure 1 shows a two-member frame ABC, with hinge at A and roller at C, exhibiting large rotations in both members under the action of an applied force P. Although each member is prismatic, the parameter r allows any relative stiffness between them. In the figure, the long-dashed line represents a possible small initial displacement u_{y0} in member AB that preserves the right angle at B. This causes an initial axial displacement in BC but does not introduce any initial transverse displacement or curvature into that member. The displacements of any point of AB are symbolized by u_x and u_y, the latter being defined as the *net* displacement. In contrast, θ, signifies the *total* inclination. The meaning of other symbols appearing in Fig. 1 is obvious.

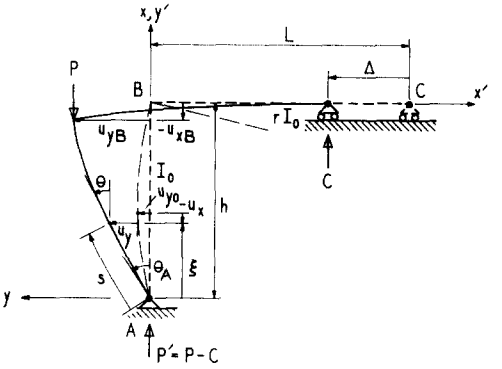

FIG. 1. A two-member frame with finite rotations.

In its buckled position, each member can be described, using the distance s as the independent variable, by three coupled, first-order, nonlinear differential equations, one arising from the Bernoulli–Euler formula and the other two from the geometry of the deflected centerline. For member AB they are:

$$\begin{aligned} \frac{d\theta}{ds} &= \frac{M}{EI_0} + K_0, \\ \frac{du_y}{ds} &= \sin\theta - \frac{du_{y0}}{ds}, \\ \frac{d\xi}{ds} &= \cos\theta, \end{aligned} \tag{1}$$

where K_0 is the initial curvature, E is Young's modulus, and M is the bending moment. For the particular frame being considered,

$$M = -(P-C)(u_y + u_{y0}). \tag{2}$$

In like manner, for BC,

$$\begin{aligned} \frac{d\theta'}{ds'} &= \frac{M'}{rEI_0}, \\ \frac{du_y'}{ds'} &= \sin\theta', \\ \frac{d\xi'}{ds'} &= \cos\theta', \end{aligned} \tag{3}$$

where a similar notation is being used but with a prime to indicate that the quantities belong to BC. For this member,

$$M' = -Pu_{yB} - C\xi'. \tag{4}$$

Equations (1) and (3), together with appropriate boundary conditions, constitute a nonlinear boundary-value problem describing the behavior of a two-member frame.

METHOD OF SOLUTION

The problem formulated in the previous section can be solved by the following "shooting" method: Convert the boundary-value problem into an initial-value problem by assuming enough initial conditions to obtain a starting point, integrate around the frame, and check the boundary conditions at the terminal point. For AB, the initial conditions are

$$\theta(0) = \theta_A, \qquad u_y(0) = 0, \qquad \xi(0) = 0, \tag{5}$$

while, for BC, they are

$$\theta'(0) = \theta_B, \qquad u_y'(0) = u_{xB}, \qquad \xi'(0) = -u_{yB}. \tag{6}$$

If P is prescribed, then two input parameters, θ_A and C, must be assumed in order to start the solution. Once this is done, the complete integration process can be effected by any of several standard numerical techniques for systems of first-order equations, including the predictor–corrector methods. The results presented in this paper were obtained by an integrating package based on the modified Euler method. The integration, as well as all the other numerical work, was carried out on an IBM 7094-7040 DCS.

The scheme for adjusting the two input parameters so as to satisfy the terminal conditions can be described by letting the input to the integrating package consist of the two independent variables:

$$x_1 = \theta_A, \qquad x_2 = C \text{ (assumed)}. \tag{7}$$

After integration, C can be recomputed by

$$C = -\frac{Pu_{yB}}{L-\Delta}, \tag{8}$$

so that the output can consist of the two functions

$$f(x_1, x_2) = u_{yC}', \qquad g(x_1, x_2) = C \text{ (recomputed)}. \tag{9}$$

The correct values for the input parameters are then the roots of the equations:

$$f(x_1, x_2) = 0, \qquad x_2 = g(x_1, x_2). \tag{10}$$

Since no derivatives of f or g are available, the specific algorithm chosen to solve system (10) is the following two-step combination of standard methods not requiring derivatives:

(i) *Regula falsi* (with interpolation only):

$$x_1^{(i+1)} = x_1^{(i)} - \frac{f(x_1^{(i)}, x_2^{(i,T)})}{m_i}, \tag{11a}$$

$$m_i = \frac{f(x_1^{(i)}, x_2^{(i,T)}) - f(x_1^{(R)}, x_2^{(R,T)})}{x_1^{(i)} - x_1^{(R)}}, \tag{11b}$$

where $x_1^{(R)}$ is the last value of $x_1^{(i)}$ such that $f(x_1^{(R)}, x_2^{(R,T)})$ has opposite sign to current $f(x_1^{(i)}, x_2^{(i,T)})$, and where $x_2^{(i,T)}$ is a temporary value of x_2 obtained for each i from step (ii).

(ii) *Iteration:*

$$x_2^{(i,j+1)} = g(x_1^{(i)}, x_2^{(i,j)}). \tag{12}$$

A discussion of the convergence properties of these methods is given by Isaacson and Keller [3].

INTERMEDIATE RESULTS

Figure 2 shows equilibrium load–deflection curves for the special case of a square frame with equal moments of inertia. In this figure, Q is a dimensionless force given by

$$Q = \frac{Ph^2}{EI_0}, \tag{13}$$

and a is the amplitude of an initial sinusoidal curvature in AB. Curves are plotted for $a/h = 0$ and for the extreme case of $a/h = 0{\cdot}1$. For intermediate values of a/h a family of curves can be visualized as lying between the two extremes and approaching the curves for $a/h = 0$ as a/h approaches zero.

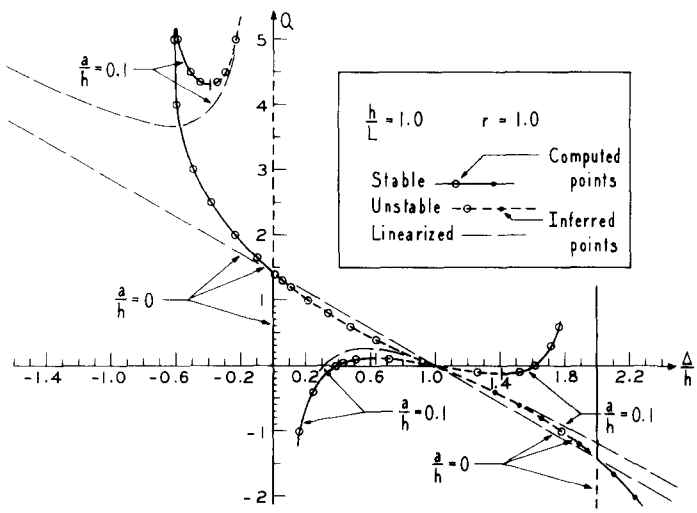

FIG. 2. Q vs. Δ curves for $a/h = 0$ and $a/h = 0{\cdot}1$.

The heavy solid lines in Fig. 2 represent stable-equilibrium paths and the heavy dashed lines unstable-equilibrium. An examination of the case $a/h = 0$ reveals that, for any point on the unstable paths, a perturbation (under constant load) that decreases Δ will cause the frame to snap back to the straight position when $Q < 1{\cdot}421$ and to a deformed position with Δ negative when $Q > 1{\cdot}421$. On the other hand, a perturbation (under constant load) that increases Δ will cause the frame to snap over onto its side, giving $\Delta/h = 2{\cdot}0$. For any point on the stable paths, a perturbation results in a return to the equilibrium position, with the exception of the two critical points where bifurcation occurs. At the critical point on the Q-axis, snap-over is imminent; at that corresponding to $\Delta/h = 2{\cdot}0$, snap-back is imminent. These critical points are examples of the "unstable bifurcation point" introduced by Koiter [4] in his small-deflection theory of post-buckling behavior.

A buckling analysis similar to the foregoing can be made also for the initial-curvature case of Fig. 2. The sensitivity of the structure to imperfections, a concept discussed by Koiter [4] for static loads and by Budiansky and Hutchinson [5] for dynamic loads, is readily apparent in this problem from the drastic reduction of load-carrying capacity caused by the initial curvature in AB.

Figure 3 shows equilibrium reaction–deflection curves for $h/L = 1{\cdot}0$ and $r = 1{\cdot}0$. Here, Q' is given by

$$Q' = \frac{P'h^2}{EI_0}, \tag{14}$$

and a is as before. Except for the string of points at $\Delta/h = 1{\cdot}0$, which will be discussed later, there is a one-to-one correspondence between points in Figs. 2 and 3.

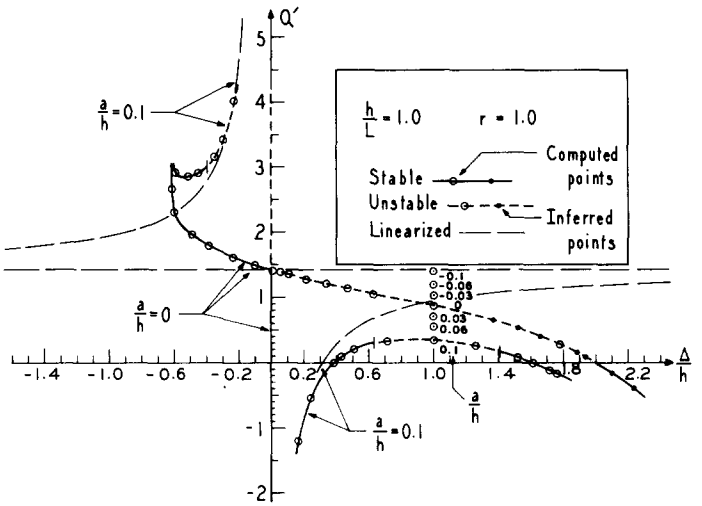

FIG. 3. Q' vs. Δ curves for $a/h = 0$ and $a/h = 0{\cdot}1$.

The long-dashed curves in Figs. 2 and 3 display the results of the classical linearized theory. For $a/h = 0$, that theory leads to an eigenvalue problem, with the lowest eigenvalue $Q' = 1{\cdot}421$. For that reaction, the deflection is indeterminate, i.e. any deflected position is an equilibrium configuration. Hence the horizontal straight line in Fig. 3. To make Q' constant, it is essential that Q vary linearly with Δ and be zero when $\Delta = L$, as in Fig. 2. The linearized curve for $a/h = 0{\cdot}1$ once again illustrates the sensitivity of the structure to imperfections.

The linearized theory is valid only for small values of $|\Delta|$ but is plotted out to large values in Figs. 2 and 3 for purposes of comparison of the "exact" solution with the linearized. Such a comparison reveals that the latter, quite by coincidence, gives fairly accurate values for Q in the entire interval $0 \leq \Delta/h \leq 1{\cdot}0$ for the case $a/h = 0$.

When $\Delta = L$, end C of the frame is directly above end A and the load P must be zero. The question arises as to what are the reactive force P' and the shape of the frame for this "squeezed" position. It is evident from equation (8) that the previous algorithm is incapable of dealing with this situation, inasmuch as the function g is not defined for $\Delta = L$. A completely new algorithm must be devised, as explained in the next section.

ANALYSIS OF "SQUEEZED" POSITION

The problem posed at the end of the last section can be solved by another "shooting" method with two input parameters. Once again, let the input to the integrating package be:

$$x_1 = \theta_A, \qquad x_2 = C, \tag{15}$$

but now let the output be:

$$f_1(x_1, x_2) = u'_{yC}, \qquad f_2(x_1, x_2) = L - \Delta. \tag{16}$$

The correct values for the input parameters are then the roots of the equations:

$$f_1(x_1, x_2) = 0, \qquad f_2(x_1, x_2) = 0. \tag{17}$$

Again, the fact that no derivatives are available governs the choice of algorithm to be used for solving system (17) and suggests as one possibility the following two-step *regula falsi:*

(i)
$$x_1^{(i+1)} = x_1^{(i)} - \frac{f_1(x_1^{(i)}, x_2^{(i,T)})}{m_i}, \tag{18a}$$

(ii)
$$x_2^{(i,j+1)} = x_2^{(i,j)} - \frac{f_2(x_1^{(i)}, x_2^{(i,j)})}{m_j}, \tag{18b}$$

where m_i and m_j are slopes of interpolating straight lines, and the other symbols have meanings similar to those ascribed to them in the previous algorithm.

Figure 3 shows seven points corresponding to various values of a/h computed by the foregoing algorithm.

Figure 4 shows the variation of Q' with r for a square frame with no initial curvature.

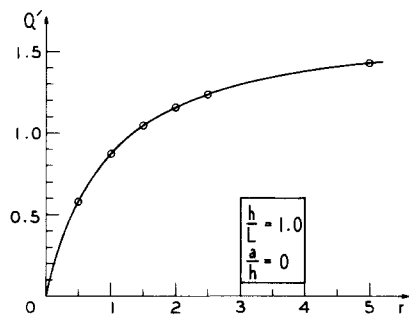

FIG. 4. Force at squeezed position vs. relative stiffness.

FINAL RESULTS AND CONCLUSIONS

The computer programs devised for this project yielded values for all three dependent variables in equations (1) and (3), their first derivatives, and certain other computed quantities such as x-displacements, at numerous points along the members. Some of these data for the case of the square frame with $r = 1{\cdot}0$ and $a/h = 0$ have been used to plot the deformed shapes of Fig. 5. Each position shown corresponds to a pair of points in Figs. 2 and 3. The "exceptional" configurations corresponding to critical load, squeezed position, and snapped-over position are included.

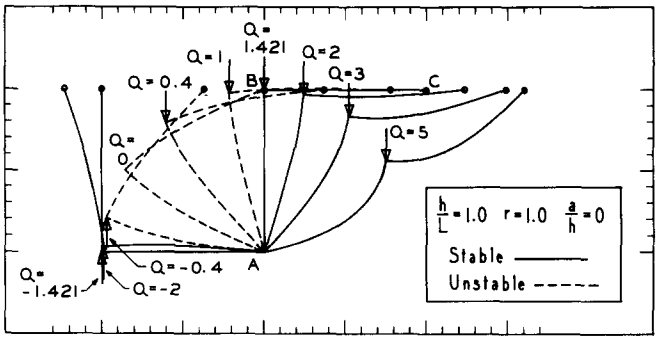

FIG. 5. Deformed shapes for various loads.

The unstable shapes are shown by dashed lines in Fig. 5. These are characterized by decreasing magnitude of successive loads with increasing displacement, or vice versa. Any one of the unstable frames will snap either left or right under a perturbation. The computing scheme was capable of predicting these unstable positions without becoming unstable itself because in effect it assumed "testing-machine" conditions, in which the vertical position of B is imposed and the load measured.

Acknowledgements—The author wishes to express his indebtedness to the Yale Computer Center and the National Science Foundation for supplying the computer time used in this research.

REFERENCES

[1] S. P. TIMOSHENKO and J. M. GERE, *Theory of Elastic Stability*, 2nd edition. McGraw-Hill (1961).
[2] JOHN V. HUDDLESTON, A numerical technique for elastica problems. In preparation.
[3] E. ISAACSON and H. B. KELLER, *Analysis of Numerical Methods*. Wiley (1966).
[4] W. T. KOITER, Elastic stability and post-buckling behavior. *Nonlinear Problems*, edited by R. E. LANGER, pp. 257–275. The University of Wisconsin Press (1963).
[5] B. BUDIANSKY and J. W. HUTCHINSON, Dynamic buckling of imperfection-sensitive structures. *Proc. 11th Int. Congr. of Applied Mechanics*, 1964, pp. 636–651.

(*Received* 3 *March* 1967; *revised* 17 *April* 1967)

Résumé—Une étude est faite du comportement au flambage d'un cadre à deux membrures, en tenant compte de rotations grandes dans le cas des deux membrures. Des algorithmes spéciaux sont conçus pour résoudre le problème de la valeur limite non linéaire qui se présente, et des solutions obtenues sur une machine à calculer digitale sont tracées et comparées à des résultats linéarisés. Des configurations d'équilibre stable et instable se distinguent, et les circonstances dans lesquelles le cadre se tourne brusquement sur son côté sont décrites.

Zusammenfassung—Das Knickbenehmen eines Zweistab-Rahmens mit freier Drehbarkeit beider Stäbe wird untersucht. Besondere Ausdrücke werden gewählt um die nichtlinearen Grenzwertsprobleme zu lösen, Lösungen die mittels Digitalrechner erhalten werden, werden mit linearisierten Resultaten verglichen. Stabile und unstabile Gleichgewichtsformen werden erkannt und die Umstände, unter welchen der Rahmen auf die Seite fällt werden beschrieben.

Абстракт—Рассматривается задача устойчивости двухстержневой рамы, в которой допускается большая вибрация в этих обоих стержнях. Выводится специальный альгоритм для расчета нели-

нейной задачи для граничных условий. Решение, которое получено с помощью вычислительных машин, вычерчивается на графике и сравнивается с решением в линейной постановке. Обсуждается стабильная и нестабильная форма равновесия. Определяются крайние расстояния прогибов рамы.